DUAL-TASK VISION TRANSFORMER FOR RAPID AND ACCURATE INTRACEREBRAL HEMORRHAGE CLASSIFICATION ON CT IMAGES

Jialiang Fan

Franklin College of Arts and Sciences
University of Georgia
Athens
jialiang.fan@uga.edu

Guoyu Lu

College of Engineering University of Georgia Athens gl72151@uga.edu

Lucan Li

School of Art
Lanzhou University
Lanzhou
lilucan1127@gmail.com

Xinhui Fan

Department of Neurology The First Hospital of Yulin Yulin fanxinhui89@foxmail.com

ABSTRACT

Intracerebral hemorrhage (ICH) is a severe and sudden medical condition caused by the rupture of blood vessels in the brain, leading to permanent damage to brain tissue and often resulting in functional disabilities or death in patients. Diagnosis and analysis of ICH typically rely on brain CT imaging. Given the urgency of ICH conditions, early treatment is crucial, necessitating rapid analysis of CT images to formulate tailored treatment plans. However, the complexity of ICH CT images and the frequent scarcity of specialist radiologists pose significant challenges. Therefore, we build a dataset from the real world for ICH and normal classification and three types of ICH image classification based on the hemorrhage location, i.e., Deep, Subcortical, and Lobar. In addition, we propose a neural network structure, i.e., dual-task vision transformer (DTViT), for the automated classification and diagnosis of ICH images. The DTViT utilizes the encoder from the Vision Transformer (ViT), employing attention mechanisms for feature extraction from CT images. Also, it incorporates two multilayer perception (MLP)-based decoders to simultaneously identify the presence of ICH and classify three types of hemorrhage locations. Experimental results demonstrate that DTViT performs well on the built real-world test dataset. The code and dataset for this work will be made publicly available upon paper acceptance at: https://github.com/Jialiangfan/ ICH-classification.

Keywords Intracerebral hemorrhage, image classification, vision transformer, transfer learning.

1 Introduction

Intracerebral hemorrhage (ICH) is a type of severe condition characterized by the formation of a hematoma within the brain parenchyma[1, 2]. Representing 10-15% of all stroke cases, ICH is linked to significant morbidity and mortality rates[3]. Head computerized tomography (CT) is the standard method to diagnose ICH that can obtain accurate images of the head anatomical structure and detect abnormalities. However, analyses of head CT images for ICH classification and diagnosis usually require skilled radiologists, who are in very short supply in developing countries or regions. This may lead to delays in setting appropriate treatment plans and interventions, which are very crucial for accurate ICH patients.

Furthermore, the diagnosis and analysis of ICH in CT images often require extensive experience and concentrated attention. However, when physicians are overworked or face a high volume of cases, misdiagnoses can inevitably occur. Therefore, the use of assistive medical technologies to aid physicians in diagnosing and analyzing ICH images can enhance the speed of diagnosis and treatment. This not only alleviates the shortage of medical resources but also improves diagnostic efficiency and accuracy, which are of significant importance to both physicians and patients.

In recent years, computer vision methods based on deep learning have played a crucial role in CT imaging diagnostics. Neural network models trained on extensive datasets of real-world data have demonstrated high accuracy and efficiency on medical images. These models can be applied to tasks such as classification[4, 5], segmentation[6, 7], or enhancement of medical images[8, 9]. For example, Sahu *et al.* [10] present an automated deep learning-based system for COVID-19 detection using chest CT images, achieving a 95.73% accuracy through advanced preprocessing and the proposed model, highlighting its efficiency over manual diagnostic methods. Huo *et al.* [11] present a general-purpose model for medical image classification that uses hierarchical multi-scale feature fusion to efficiently extract and integrate local and global features, significantly enhancing lesion detection in medical imagery. Huynh *et al.* [12] introduces a loss function named adaptive alended consistency loss for semi-supervised medical image learning that addresses class imbalance by blending class distributions, demonstrating superior performance over existing methods in experiments on imbalanced datasets.

There are also numerous studies that have utilized computer vision and deep learning techniques for ICH image detection and classification to aid medical professionals and enhance diagnostic efficiency[13, 14]. In literature [13], a deep learning model based on ResNet and EfficientDet that detects bleeding in CT scans is proposed, offering both classification and region-specific decision insights and achieving an accuracy of 92.7%. Literature [14] demonstrates the efficacy of convolutional neural network (CNN)-based deep learning models, particularly CNN-2 and ResNet-50, in classifying strokes from CT images, with future plans to optimize these models for improved diagnostic accuracy and efficiency. Li *et al.*[15] propose propose a Unet-based neural network model to detect hemorrhage strokes of CT images, achieving an accuracy of 98.59%. However, these studies primarily focus on the task of classifying whether there is cerebral hemorrhage, neglecting further detection and diagnosis, i.e., the location and depth of the hemorrhage, which is more clinically significant.

The Transformer, a network architecture based on the self-attention mechanism, has achieved remarkable success in the field of natural language processing (NLP) in recent years[16]. Building on this success, researchers have extended the Transformer to the field of computer vision, introducing Vision Transformer (ViT)[17]. The ViT model segments images into patches and feeds them into the Transformer architecture. Then, computes attention weights between different pixel blocks, facilitating effective feature extraction from images. Experimental results demonstrate that Vision Transformers achieve superior and more promising performance compared to traditional CNN-based neural networks.

Transfer learning is widely used in deep learning to reduce training time and improve training efficiencies. A pre-trained model is firstly built on a large benchmark dataset such as ImageNet[18], and common features are captured and saved in the weights of models. When applying the model to a new dataset or different tasks, we can train the model using task-specific datasets on top of the pre-trained model. Transfer learning also reduces the need for large labeled datasets, making deep learning on small or imbalanced datasets possible, which is particularly suitable for medical images.

Building on the aforementioned discussions, we first build an image dataset from real-world sources that includes head images of both healthy individuals and ICH patients, categorized into three types—Deep, Lobar, and Subtentorial—based on the location of the hemorrhage. Furthermore, a dual-task Vision Transformer (DTViT) is designed to simultaneously classify images of normal individuals and ICH patients, as well as categorize three types of ICH based on the hemorrhage location. We conduct experiments using the built dataset and the proposed model, and the results show that our proposed model achieves superior testing accuracy of 99.88%. The contributions of this paper are summarized as follows:

- We have constructed a real-world ICH image dataset comprising CT images of both normal individuals and
 patients classified into three types of ICH, addressing issues of insufficient brain hemorrhage image datasets
 and the lack of datasets for brain hemorrhage location, which is of great significance to both medical and
 computer vision research.
- Built upon the constructed dataset, We have developed a deep learning model, i.e., dual-task Vision Transformer (DTViT), which is capable of performing dual-classification tasks simultaneously: distinguishing CT images of normal and ICH patients and identifying the type of ICH according to the hemorrhage location.
- Our comparative experiments show that the DTViT model achieves 99.88% accuracy, outperforming existing CNN models and demonstrating the high quality of our dataset.

The remainder of this paper is structured as follows: Section 2 describes the dataset, data preprocessing techniques, and the architecture of DTViT. Section 3 details the experimental setup, evaluation metrics, and the results obtained. Section 4 discusses the limitations of this study and directions for future research. Finally, Section 5 concludes the paper.

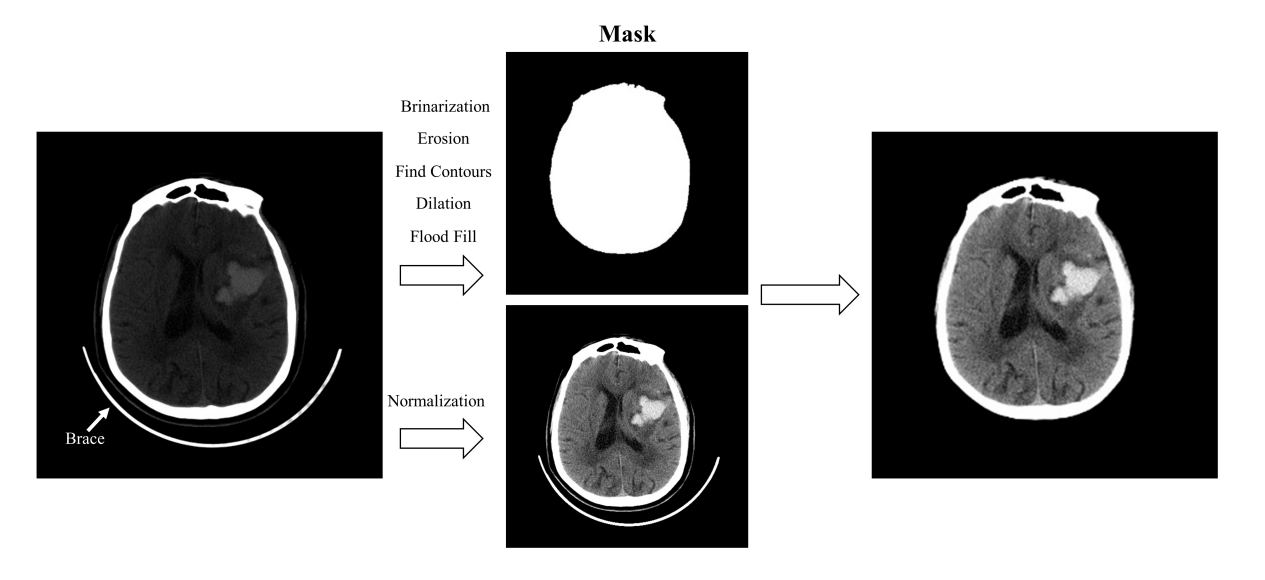


Figure 1: Morphological treatment of CT images.

2 Materials and methods

In this section, we introduce the dataset, the data preprocessing of ICH images, and the construction of DTViT.

2.1 Dataset

The dataset is sourced from the Department of Neurology at The First Hospital of Yulin. It includes 15,936 CT slices from 249 patients with intracerebral hemorrhage (ICH) collected between 2018 and 2021, and 6,445 CT slices from 199 healthy individuals from 2024. The healthy subjects have one set of CT images, while the ICH patients have two sets, captured within 24 hours and within 72 hours of symptom onset. All images were obtained using the LightSpeed VCT scanner from GE, USA, at Yulin First Hospital. All scans are saved as DCM files, featuring a resolution of 512×512 pixels, a slice thickness of 5 mm, and an inter-slice gap of either 5 mm or 1 mm.

In addition, each group of ICH images are manually classified into three different types according to hemorrhage location by physician: Deep ICH, Lobar ICH, and Subtentorial ICH. To protect patient's privacy, the dataset only includes patients' gender and CT images. A detailed data description is listed in Table 1.

Attribute	Total	Value	Number	Percentage
Sex	221	Male	117	52.94%
		Female	104	47.06%
ICH	12651	Yes	8244	65.16%
		No	4407	34.84%
Hemorrhage Location	8244	Deep	6093	73.91%
		Lobar	1656	20.09%
		Subtentorial	495	6%

Table 1: Data distribution of the dataset.

2.2 Data preprocessing

The data preprocessing is composed of three stages: morphological treatment, manual filtering, and data augmentation.

2.2.1 Morphological treatment

When taking CT images, patients are equipped with fixation braces to keep their heads steady, which is also captured by the scanner and may add noise to the image data. Therefore, it is necessary to remove the artifact to purify the data. We apply morphological processing to remove the fixation brace and normalize the images, converting them from DICOM to JPG format. The steps are as follows.

Initially, the pixel array is extracted from the DICOM file and duplicated twice. The first duplicate is used to create a mask, while the second is for generating the final result. We start by binarizing the pixel array to emphasize key features and apply erosion using a disk-shaped element to minimize noise. Next, the edge columns are zeroed out to remove potential artifacts, and flood filling is performed to enhance specific areas, thus producing the mask image.

Subsequently, this mask is applied to the second, normalized pixel array. The resulting image is then converted to 8-bit integers and saved as a JPG file. An instance of the original CT image and the processed result is displayed in Fig. 1. It can be seen that the fixed brace has been successfully removed and the normalized image is much clearer than the original.

2.2.2 Manual filtering

The head CT scan usually starts from the base of the brain (near the neck) and covers the entire brain up to the forehead. It means that only part of CT scans can capture the hemorrhage location and present a clear view for diagnoses, and other CT images do not include effective information and are useless for classification. Therefore, medical specialists manually diagnose and select each group of CT images to remove meaningless images to refine the dataset and reduce noise. This step is critical to constructing the dataset.

2.2.3 Data augumentation

As presented in Table 1, The number of images for three types of cerebral hemorrhage locations varies significantly. Therefore, we take data augmentation operation on subtentorial type CT images. Firstly, we augmented the dataset of three types of cerebral hemorrhage CT images proportionally to ensure that the distribution was approximately 1:1:1. Secondly, we also augmented the images without cerebral hemorrhage to achieve a roughly 1:1 ratio between the two categories. The augmented dataset consists of 30,222 images in total, including 13,221 normal images and 17,001 ICH images, which are further categorized into 6,093 Deep, 5,940 Lobar, and 4,968 Subtentorial images. Furthermore, to enhance the diversity of the dataset, we applied image transformation on the training dataset, including center cropping to the size of 224x224, random rotation of 15 degrees, random sharpness adjustment with a factor of 2, and normalization with the mean value [0.485, 0.456, 0.406] and standard deviation [0.229, 0.224, 0.225].

2.3 Methods

This section introduces the construction of DTViT. Firstly, we introduce the basics of the Vision Transformer and the architecture of DTViT. Then, the transfer learning and details of the pre-trained model are introduced. An overall diagram is shown in Fig. 2.

2.3.1 Structure of DTViT

In ViT, a raw 2D image is initially transformed into a sequence of 1D patch embeddings, which mirrors the word embedding technique used in natural language processing. Similarly, the positional embeddings are applied to the constructed patch embeddings to retain information about the location of each patch in the original image. Then, the sequences are fed into the encoder of the Transformer, which consists of multi-head self-attention layers and MLP layers, with normalization and residual connections. This enables the model to capture intricate connections among different patch blocks. Finally, the output is processed by the decoder, i.e., the full-connection layer or MLP layer, to output the classification results. The architecture of the ViT encoder is depicted in Fig. 2.

Considering the high-density shadows, variable scales, and diverse locations characteristic of ICH CT images, we adopt the ViT's encoder to the DTViT. Additionally, two MLP-based decoders have been integrated into the DTViT as decoders to achieve dual-task classification. As shown in Fig. 2, Two decoders share the feature extraction results from the encoder, where the MLP classifier 1 achieves the classification of whether there is a hemorrhage in the image, and the MLP classifier 2 classifies the type of hemorrhage based on the location information extracted by the encoder.

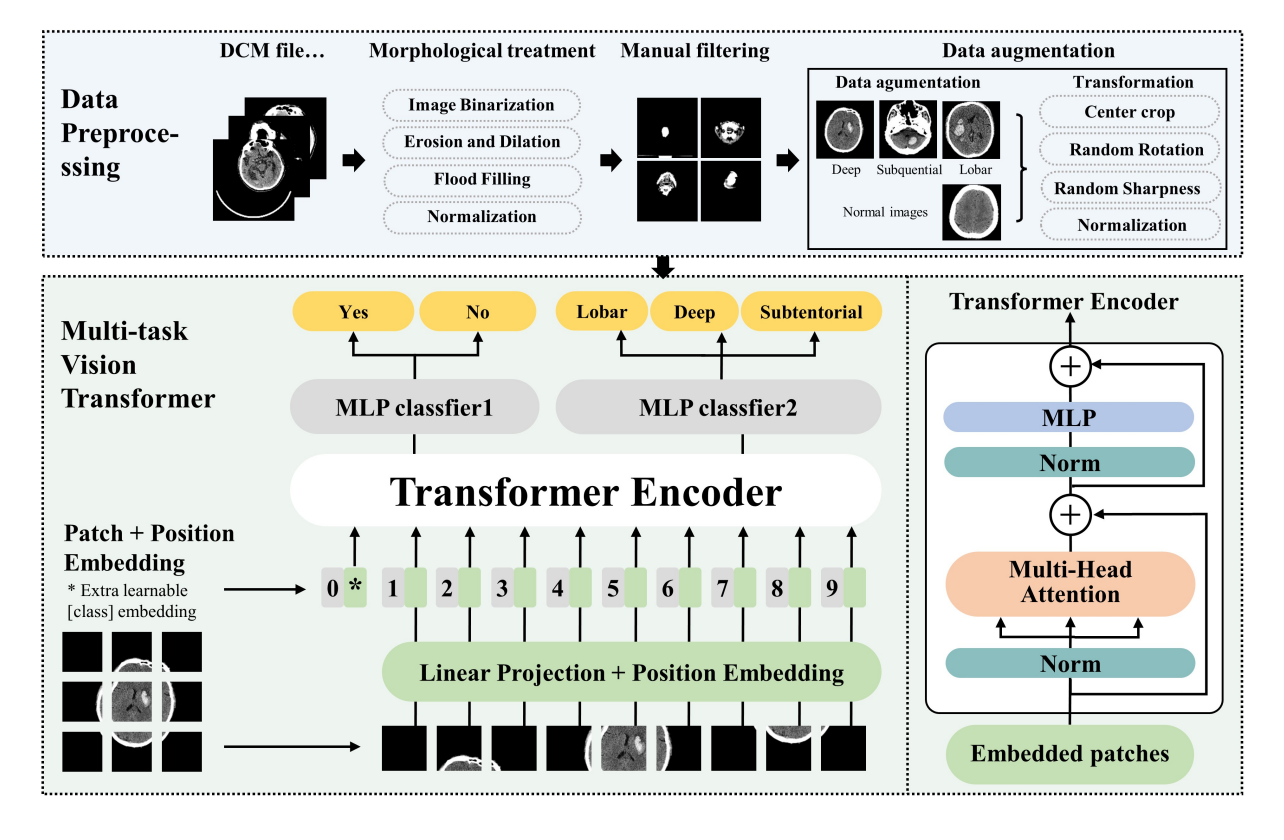


Figure 2: CT image filtering. (a) The original CT image with a fixation device. (b) Processed image with fixation device removed.

2.3.2 Transfer learning

Transfer learning refers to training a model that has already been pre-trained on another large dataset, such as ImageNet[18]. This approach can significantly save time and enhance training efficiency. It allows the model to leverage previously learned features and knowledge, which is especially useful when dealing with similar but new tasks. Therefore, we train the DTViT based on the pre-trained Vision Transformer encoder[19] and fine-tune the model's parameters.

Specifically, there are three types of pre-trained ViT models: ViT-Base, ViT-Large, and ViT-Huge. The ViT-Base model, with its 12 blocks, is suitable for datasets of moderate complexity. The ViT-Large model, which has 24 blocks and larger embedding dimensions, offers better performance but requires more computational resources. The ViT-Huge is the largest one of the three models, taking 32 blocks and being suitable for high-complex tasks. For our work with DTViT, we use the ViT-Large as the pre-trained model[20], which is trained on ImageNet-1K[18]. The configuration of the pre-trained model is shown in Table 2.

Table 2: Configuration and Parameters of ViT-Large Model.

Configuration	Value		
Patch Size	16		
Embedding Dimension	1024		
Attention Heads	16		
MLP Dimension	4096		
Parameters	304326632		

3 Experiments

In this section, we conduct experiments using the built dataset with and without data augmentation to validate the dataset and get the performance of the DTViT. The experiment environment and parameters used in the training process are first given. Then, we introduce several evaluation indices used in experiments. Further, we present the accuracies and losses of datasets. In addition, we apply the dataset to classical CNN models for comparison to depict the performance of our model.

3.1 Environments and parameters

The experimental hardware setup is as follows: The CPU used is an AMD Ryzen 5975WX with 32 cores, and the GPU is an NVIDIA RTX 4090 equipped with 24 GB of memory. The operating system is Ubuntu 20.04. CUDA version 12.3 was utilized for computation. All experiments were conducted using Python version 3.8.18 and PyTorch version 2.3.0.

Additionally, we utilized the AdamW optimizer[21] with an initial learning rate of 2×10^{-5} and a weight decay of 0.01. The batch size is set as 8 for the training data without data augmentation, 32 for the training data with data augmentation, 32 for the validating data, and 4 for the testing data. The model was trained over 10 epochs. We employed the cross-entropy function as the loss function to optimize the model's performance.

3.2 Evaluation indices

We have taken various experiments and adopted several models to get the performance of DTViT. Firstly, the correct classification of images, i.e., the accuracy, is the criterion of the model performance, which is presented as

$$Accuracy = \frac{TP + TN}{TP + TN + FP + FN},\tag{1}$$

where TP represents true positive instances; TN represents true negative instances; FP represents false positive instances; FN represents false negative instances. The precision metric represents the proportion of correctly predicted positive instances out of all the instances predicted as positive in a class. Precision is determined using the following equation:

$$Precision = \frac{TP}{TP + FP}. (2)$$

The recall metric quantifies the proportion of positive instances that are correctly identified and the corresponding formula to calculate recall is presented as

$$Recall = \frac{TP}{TP + TN}. (3)$$

The sensitivity metric calculates the proportion of positive instances that are correctly classified, which is defined as

$$Sensitivity = \frac{TP}{TP + TN}. (4)$$

In addition, the F1-score metric is the harmonic mean of precision and recall. It is computed as

$$F1 = \frac{2 * (Precision * Recall)}{Precision + Recall}.$$
 (5)

In medical fields, specificity is a good evaluation index to guarantee that individuals who do not have the disease are not wrongly diagnosed, thereby avoiding unnecessary treatment and anxiety. The calculation of specificity is presented as

$$Specificity = \frac{TN + FP}{TN}. (6)$$

We take these indices to evaluate the performances of DTViT on the built dataset with and without data augmentation.

3.3 DTViT performances

Figure 3 illustrates the evolution of losses and accuracies during training and validating processes, both with and without data augmentation. As depicted in Fig. 3(a), training and validating losses decrease steadily throughout the process, eventually stabilizing at approximately 0.01. Correspondingly, both training and validating accuracies show steady increases, converging approximately to 0.997 by the end of the training period. By contrast, results from the non-augmented dataset display inconsistency: while training loss decreases continuously to a desirable value, the

validating loss fails to converge to the same level, ending around 0.08 and indicating overfitting. Similarly, the validating accuracy does not reach the level of the training accuracy, suggesting poor performance on unseen data.

Further, we evaluate the trained model on the test dataset to get the DTViT's performance on the unknown data, which is composed of 1266 CT images, including 459 for normal images and 807 ICH images with Deep 595, Lobar 163, and Subtentorial 49. Confusion matrixes are shown in Fig. 4, where Fig. 4(a) shows the result of Task 1 for normal and ICH patients classification, and Fig. 4(b) shows the results of Task 2 for three types of ICH classification. It can be seen that almost all positive and negative cases on the test dataset are classified correctly, except 1 normal image is misclassified as an ICH image. Similarly, the classification of ICH types also achieved excellent results with a testing accuracy of 0.996. In detail, evaluation indices of precision, recall, F1 score, and specificity are displayed in Table 3.

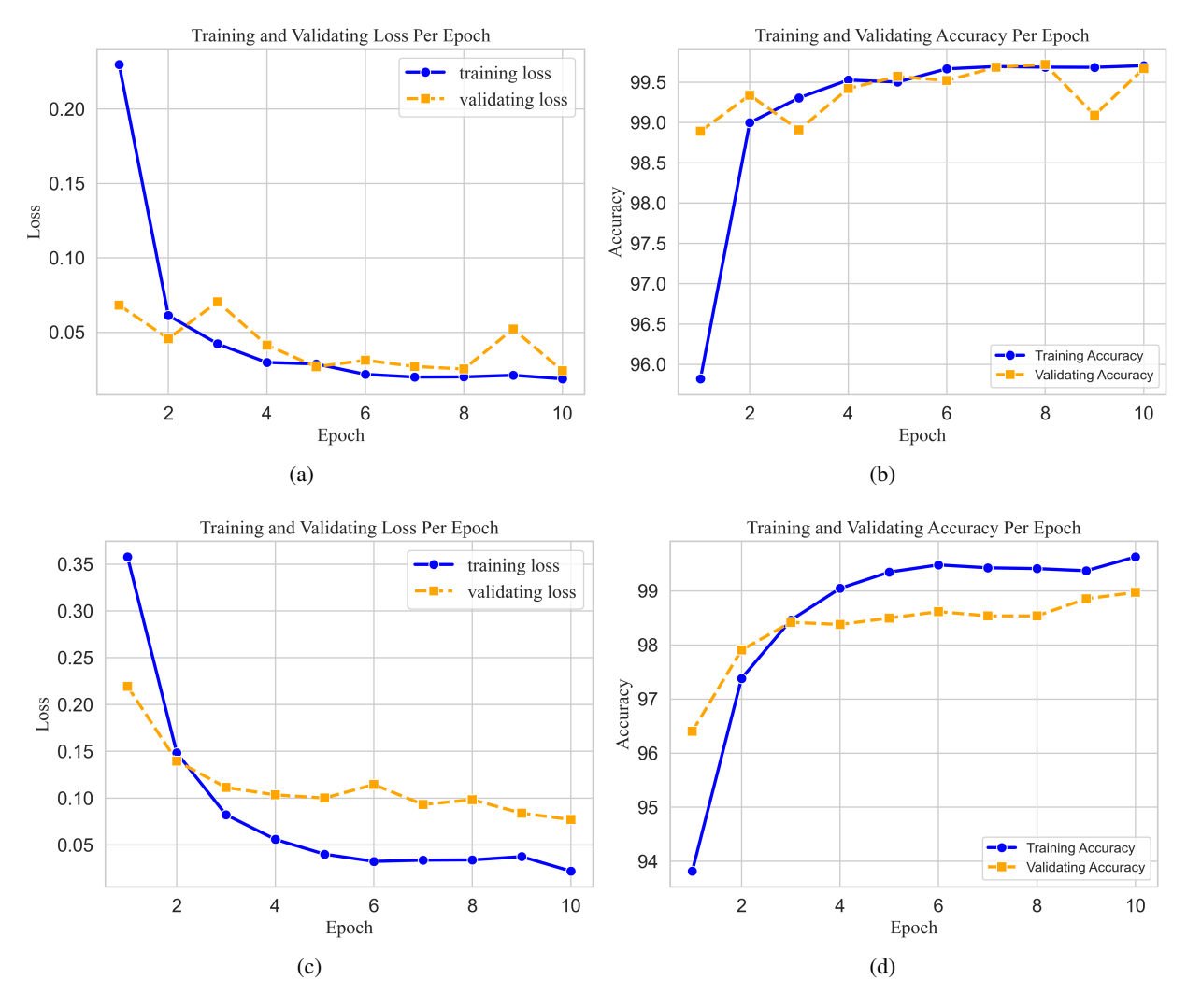


Figure 3: The accuracy and loss curves in training and validating processes on datasets with and without augmentation. (a) Training and validating losses with augmentation. (b) Training and validating accuracies with augmentation. (c) Training and validating losses without augmentation. (d) Training and validating accuracies without augmentation.

3.4 Comparative experiments

To better demonstrate the performance of the DTViT, we conducted comparative experiments using classical CNN models, including ResNet18[22], AlexNet[23], SqueezeNet[24], and DenseNet[25] on our augmented dataset. The comparative results are shown in Table 4. Specifically, the proposed model, i.e. DTViT, achieves the lowest loss of 0.0102 and the highest accuracy of 0.9988 over these models. In addition, the DTViT also ranks first on other evaluation metrics, except its precision is slightly lower than DenseNet's.

Table 3: Performance comparison of DTViT with and without data augmentation on the testing dataset.

Classifier	DA	Accuracy	Precision	Recall	F1 Score	Specificity
Classifier 1	Yes	1	1	1	1	1
Classifier 1	No	0.996	0.991	1	0.995	0.995
Classifier 2	Yes	0.996	0.998	0.997	0.997	1
Classifier 2	No	0.992	0.994	0.996	0.995	0.995

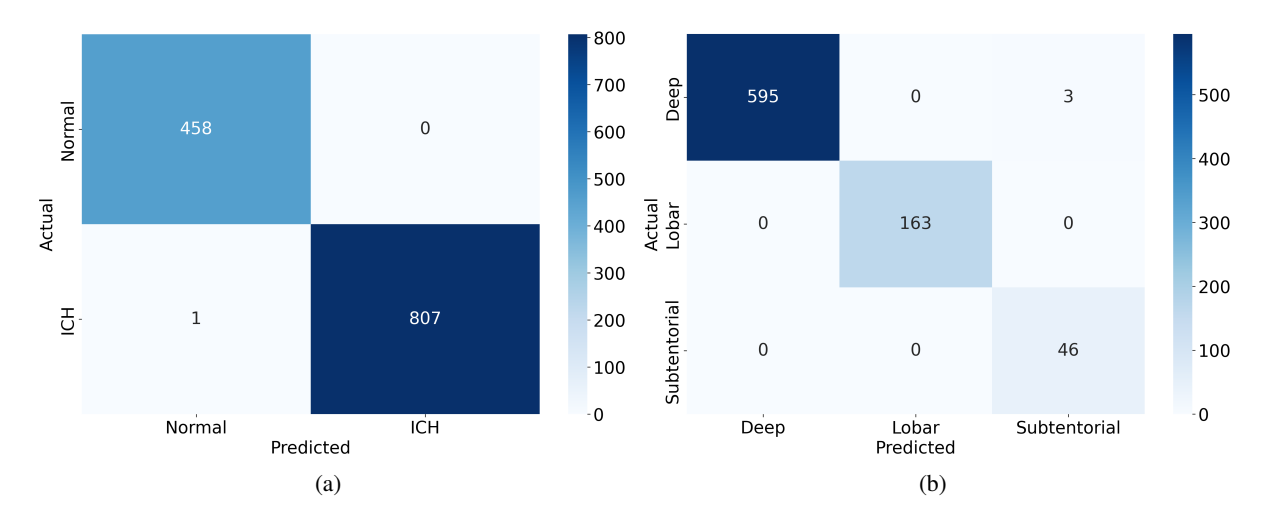


Figure 4: Confusion matrixes of DTViT for two classification tasks on the testing dataset. (a) Confusion matrix of task 1 for normal and ICH classification. (b) Confusion matrix of Task 2 for three types of ICH classification.

4 Discussion

In this paper, we first collect CT images from intracerebral haemorrhage (ICH) patients and normal people, which are sourced from real-world patient data from Yulin First Hospital, China. Furthermore, medical specialists put effort into data filtering and labelling of three types of ICH haemorrhage.

Based on the built dataset, we propose the dual-task vision transformer (DTViT) model based on the vision transformer for dual-task classification. The proposed model is composed of an encoder to extract information from CT images and two decoders for different classification tasks, i.e., classification of normal and ICH images and classification of three types of ICH based on the location of the hematoma. The proposed DTViT achieves 99.7% of the training accuracy and 99.88% of the testing accuracy on the augmented dataset. We also compared the proposed model with several state-of-the-art models, i.e., Resnet18, SqueezeNet, and Alexnet, and the results show that our model achieves the best performance over these models.

There is some previous research focusing on ICH classification or detection[26, 13, 14, 27]. For example, literature[26] proposes an ICH classification and localization method using a neural network model, achieving the accuracy of 97.4%, while the input signals are microwave signals and the hardware requirements are relatively high. Also, a CT-image-based deep learning method is proposed in [13], which is based on the EfficientDet and achieves an accuracy of 92.7%. Similar work using computer vision methods for ICH detection and classification includes [28, 29], where literature [28] achieves ICH classification using a CNN-based architecture called EfficientNet; literature [29] uses ResNet-18 for ICH classification with the accuracy 95.93%.

However, to the best of our knowledge, there is neither such a dataset describing the location of hematoma of ICH CT images nor such classification model simultaneous determining whether a CT image is of a cerebral hemorrhage or normal, and classifies the three types of cerebral hemorrhage.

The primary aim of creating the Intracerebral Hemorrhage (ICH) CT image dataset and developing the classification model is to harness state-of-the-art computer vision technology to assist physicians in diagnosing and treating patients with cerebral hemorrhage. Cerebral hemorrhage is a severe, acute medical condition affecting approximately two million individuals annually, often associated with higher mortality and morbidity and limited treatment options. Early

Table 4: Overall performance comparisons with existing models.

Model	Loss	Accuracy	Precision	Recall	F1 Score	Specificity
Proposed	0.0102	0.9988	0.9991	0.9983	0.9987	1
ResNet18[22]	0.0170	0.9984	0.9989	0.9983	0.9986	0.9993
AlexNet[23]	0.0142	0.9976	0.9989	0.9983	0.9986	0.9994
SqueezeNet[24]	0.1244	0.9775	0.990	0.9889	0.9895	0.9993
DenseNet[25]	0.0119	0.9976	1	0.9964	0.9981	1

diagnosis and tailored treatment strategies based on the hemorrhage location are crucial for patient outcomes, as different hemorrhage sites require varied treatment approaches. Therefore, the classifier developed in this study, which categorizes hemorrhage based on its location, is clinically significant as it aids healthcare professionals in quickly and accurately determining treatment plans.

Limitations: This study faces several limitations. First, the dataset, derived from real clinical data, is challenging to obtain and inherently imbalanced, which may limit the model's accuracy and generalizability. Future efforts will focus on expanding and balancing the dataset through continued data collection. Second, the current data augmentation technique involves mere replication of the dataset. Future improvements will explore the use of generative models, such as diffusion models, for data enhancement.

Future Directions: In subsequent work, we aim to develop a multimodal diagnostic dataset for cerebral hemorrhage, integrating clinical data such as blood pressure, lipid profiles, and bodily element levels to enhance diagnostic accuracy. Furthermore, we plan to create a cerebral hemorrhage classification and diagnosis model based on Artificial Intelligence-Generated Content (AIGC), which will improve diagnostic efficiency for physicians.

5 Conclusion

In this paper, we have constructed a dataset for Intracerebral Hemorrhage (ICH) based on real-world clinical data. The dataset comprises CT images that have been initially processed and manually classified by medical experts into categories of normal and ICH images. Moreover, the ICH images have been categorized into three types, Subcortical, and Lobar, according to the hemorrhage's location.

Additionally, we have introduced a dual-task vision Transformer (DTViT) aimed at the classification of Intracerebral hemorrhage. This innovative neural network model incorporates an encoder, which utilizes the cutting-edge vision Transformer architecture, and two decoders that are designed to classify images as ICH or normal and to determine the hemorrhage type. Our experiments have demonstrated that the DTViT has achieved a remarkable accuracy rate of 99.88% on the test data. We have also compared the DTViT with traditional models such as Resnet18, SqueezeNet, and Alexnet.

To our knowledge, this research is the first to have developed both a specialized dataset and a neural network model tailored for hemorrhage location classification in a clinical context. This contribution holds substantial potential for enhancing clinical diagnosis and treatment planning.

Acknowledgments

This was supported in part by the University of Georgia, and in part by the Department of Neurology, The First Hospital of Yulin.

References

- [1] James M Gebel and Joseph P Broderick. Intracerebral hemorrhage. Neurologic clinics, 18(2):419–438, 2000.
- [2] Airton Leonardo de Oliveira Manoel. Surgery for spontaneous intracerebral hemorrhage. *Critical Care*, 24(1):45, 2020.
- [3] Yingfeng Wan, Katherine G Holste, Ya Hua, Richard F Keep, and Guohua Xi. Brain edema formation and therapy after intracerebral hemorrhage. *Neurobiology of disease*, 176:105948, 2023.

- [4] Hee E Kim, Alejandro Cosa-Linan, Nandhini Santhanam, Mahboubeh Jannesari, Mate E Maros, and Thomas Ganslandt. Transfer learning for medical image classification: a literature review. *BMC medical imaging*, 22(1):69, 2022.
- [5] Huiyan Jiang, Zhaoshuo Diao, Tianyu Shi, Yang Zhou, Feiyu Wang, Wenrui Hu, Xiaolin Zhu, Shijie Luo, Guoyu Tong, and Yu-Dong Yao. A review of deep learning-based multiple-lesion recognition from medical images: classification, detection and segmentation. *Computers in Biology and Medicine*, 157:106726, 2023.
- [6] Victor Ion Butoi, Jose Javier Gonzalez Ortiz, Tianyu Ma, Mert R Sabuncu, John Guttag, and Adrian V Dalca. Universeg: Universal medical image segmentation. In *Proceedings of the IEEE/CVF International Conference on Computer Vision*, pages 21438–21451, 2023.
- [7] Feiniu Yuan, Zhengxiao Zhang, and Zhijun Fang. An effective cnn and transformer complementary network for medical image segmentation. *Pattern Recognition*, 136:109228, 2023.
- [8] Jun Ma, Yuanzhi Zhu, Chenyu You, and Bo Wang. Pre-trained diffusion models for plug-and-play medical image enhancement. In *International Conference on Medical Image Computing and Computer-Assisted Intervention*, pages 3–13. Springer, 2023.
- [9] Chunming He, Kai Li, Guoxia Xu, Jiangpeng Yan, Longxiang Tang, Yulun Zhang, Yaowei Wang, and Xiu Li. Hqg-net: Unpaired medical image enhancement with high-quality guidance. *IEEE Transactions on Neural Networks and Learning Systems*, 2023.
- [10] Hemlata P. Sahu and Ramgopal Kashyap. Fine_denseiganet: Automatic medical image classification in chest ct scan using hybrid deep learning framework. *International Journal of Image and Graphics*, 0(0):2550004, 0.
- [11] Xiangzuo Huo, Gang Sun, Shengwei Tian, Yan Wang, Long Yu, Jun Long, Wendong Zhang, and Aolun Li. Hifuse: Hierarchical multi-scale feature fusion network for medical image classification. *Biomedical Signal Processing and Control*, 87:105534, 2024.
- [12] Tri Huynh, Aiden Nibali, and Zhen He. Semi-supervised learning for medical image classification using imbalanced training data. *Computer methods and programs in biomedicine*, 216:106628, 2022.
- [13] Luis Cortés-Ferre, Miguel Angel Gutiérrez-Naranjo, Juan José Egea-Guerrero, Soledad Pérez-Sánchez, and Marcin Balcerzyk. Deep learning applied to intracranial hemorrhage detection. *Journal of Imaging*, 9(2):37, 2023.
- [14] Yung-Ting Chen, Yao-Liang Chen, Yi-Yun Chen, Yu-Ting Huang, Ho-Fai Wong, Jiun-Lin Yan, and Jiun-Jie Wang. Deep learning—based brain computed tomography image classification with hyperparameter optimization through transfer learning for stroke. *Diagnostics*, 12(4):807, 2022.
- [15] Lu Li, Meng Wei, BO Liu, Kunakorn Atchaneeyasakul, Fugen Zhou, Zehao Pan, Shimran A Kumar, Jason Y Zhang, Yuehua Pu, David S Liebeskind, et al. Deep learning for hemorrhagic lesion detection and segmentation on brain ct images. *IEEE journal of biomedical and health informatics*, 25(5):1646–1659, 2020.
- [16] Ashish Vaswani, Noam Shazeer, Niki Parmar, Jakob Uszkoreit, Llion Jones, Aidan N Gomez, Łukasz Kaiser, and Illia Polosukhin. Attention is all you need. *Advances in neural information processing systems*, 30, 2017.
- [17] Alexey Dosovitskiy, Lucas Beyer, Alexander Kolesnikov, Dirk Weissenborn, Xiaohua Zhai, Thomas Unterthiner, Mostafa Dehghani, Matthias Minderer, Georg Heigold, Sylvain Gelly, et al. An image is worth 16x16 words: Transformers for image recognition at scale. *arXiv preprint arXiv:2010.11929*, 2020.
- [18] Jia Deng, Wei Dong, Richard Socher, Li-Jia Li, Kai Li, and Li Fei-Fei. Imagenet: A large-scale hierarchical image database. In 2009 IEEE conference on computer vision and pattern recognition, pages 248–255. Ieee, 2009.
- [19] Ross Wightman. Pytorch image models. https://github.com/rwightman/pytorch-image-models, 2019.
- [20] Hugo Touvron, Matthieu Cord, Matthijs Douze, Francisco Massa, Alexandre Sablayrolles, and Hervé Jégou. Training data-efficient image transformers & distillation through attention. In *International conference on machine learning*, pages 10347–10357. PMLR, 2021.
- [21] Ilya Loshchilov and Frank Hutter. Decoupled weight decay regularization. *arXiv preprint arXiv:1711.05101*, 2017.
- [22] Kaiming He, Xiangyu Zhang, Shaoqing Ren, and Jian Sun. Deep residual learning for image recognition. In *Proceedings of the IEEE conference on computer vision and pattern recognition*, pages 770–778, 2016.
- [23] Alex Krizhevsky, Ilya Sutskever, and Geoffrey E Hinton. Imagenet classification with deep convolutional neural networks. *Advances in neural information processing systems*, 25, 2012.
- [24] Forrest N Iandola, Song Han, Matthew W Moskewicz, Khalid Ashraf, William J Dally, and Kurt Keutzer. Squeezenet: Alexnet-level accuracy with 50x fewer parameters and 0.5 mb model size. *arXiv preprint arXiv:1602.07360*, 2016.

- [25] Gao Huang, Zhuang Liu, Laurens Van Der Maaten, and Kilian Q Weinberger. Densely connected convolutional networks. In *Proceedings of the IEEE conference on computer vision and pattern recognition*, pages 4700–4708, 2017.
- [26] Qinwei Li, Lunxiao Wang, Xiaoguang Lu, Dequan Ding, Yang Zhao, Jianwei Wang, Xinze Li, Hang Wu, Guang Zhang, Ming Yu, et al. Classification and location of cerebral hemorrhage points based on sem and ssa-ga-bp neural network. *IEEE Transactions on Instrumentation and Measurement*, 2024.
- [27] Nicolas Raposo, Maria Clara Zanon Zotin, David J Seiffge, Qi Li, Martina B Goeldlin, Andreas Charidimou, Ashkan Shoamanesh, Hans Rolf Jäger, Charlotte Cordonnier, Catharina JM Klijn, et al. A causal classification system for intracerebral hemorrhage subtypes. *Annals of neurology*, 93(1):16–28, 2023.
- [28] Aniwat Phaphuangwittayakul, Yi Guo, Fangli Ying, Ahmad Yahya Dawod, Salita Angkurawaranon, and Chaisiri Angkurawaranon. An optimal deep learning framework for multi-type hemorrhagic lesions detection and quantification in head ct images for traumatic brain injury. *Applied Intelligence*, pages 1–19, 2022.
- [29] Miguel Altuve and Ana Pérez. Intracerebral hemorrhage detection on computed tomography images using a residual neural network. *Physica Medica*, 99:113–119, 2022.